Distribution of seismic wave speed changes associated with the 12 May 2008 Mw 7.9 Wenchuan earthquake

Jiu Hui Chen,[1] Bérénice Froment,[2] Qi Yuan Liu,[1] and Michel Campillo[2]

Received 4 July 2010; accepted 12 July 2010; published 17 September 2010.

[1] We used continuous recordings in Sichuan, China to track the temporal change of the seismic wave speed at a regional scale, for 2 years including the Wenchuan Mw 7.9 earthquake. The data are recorded by a temporary network of 156 broad-band seismographs in a region that covers the southern 2/3 of the fault activated during the earthquake. A doublet analysis applied on the codas of seismic noise cross correlation functions is used to detect temporal velocity changes. We found clear evidence that the seismic velocity drops by up to 0.08% in the fault region just after the earthquake with fluctuations within 0.02% before the earthquake. We compared the measurements in different sub-arrays to get a spatial distribution of the velocity changes. This distribution is consistent with the volumetric strain change during the Wenchuan earthquake and shows that the co-seismic velocity change is not controlled by the response of sediments.
Citation: Chen, J. H., B. Froment, Q. Y. Liu, and M. Campillo (2010), Distribution of seismic wave speed changes associated with the 12 May 2008 Mw 7.9 Wenchuan earthquake, *Geophys. Res. Lett.*, *37*, L18302, doi:10.1029/2010GL044582.

1. Introduction

[2] On 12 May 2008, a Mw 7.9 earthquake struck Wenchuan, Beichuan and Qingchuan counties, China along the eastern margin of the Tibetan Plateau [*Burchfiel et al.*, 2008; *Zhang et al.*, 2010]. Surface geology surveys indicate a 240 km long rupture zone [*Xu et al.*, 2009]. Seismological data indicate that the rupture initiated in the southern Longmen Shan (LMS) (Figure 1) and propagated unilaterally northeastward on a northwest dipping fault for more than 320 km [*Ji and Hayes*, 2008]. Aftershock relocation results [*Chen et al.*, 2009] show that the dipping angle of the fault zone is 70° ~ 80° near the surface and is 30° ~ 60° near the hypocenter (14 ~ 19 km depth). *Shen et al.* [2009] built a comprehensive source model from GPS and InSAR data and confirmed the seismological observations.

[3] Physical processes that accompany earthquakes, such as co-seismic stress changes, the migration of fluids and the formation of damage zones in the shallow layers, can cause changes in mechanical properties of nearby crustal material. Recently, technical and methodological developments have shown that such changes in material properties can be detected. Among them, ambient noise monitoring approaches [e.g., *Sens-Schönfelder and Wegler*, 2006; *Wegler et al.*, 2009; *Brenguier et al.*, 2008a , 2008b], which use the coda of the noise correlation functions (NCFs), are specifically designed for continuous monitoring of temporal change in elastic properties of the medium (seismic wave speed), without repeating earthquakes or active sources. These studies are all relying on the extraction of the Earth response between two points from the correlation of seismic noise records [*Shapiro and Campillo*, 2004]. The nature of the later part of the NCF was analyzed by *Stehly et al.* [2008] who demonstrated that it contains at least partially the coda of the Green function. It was verified experimentally with ultrasound that the coda of the NCF can be used for monitoring the velocity changes [*Hadziioannou et al.*, 2009]. The temporal change is obtained by applying the doublet method (proposed for earthquake records by *Poupinet et al.* [1984]) on the correlation codas.

[4] In October, 2006, that is, well before the Mw 7.9 Wenchuan earthquake, Institute of Geology of the China Earthquake Administration deployed almost 300 broadband stations in western Sichuan province, covering 2/3 of the fault system activated during the Wenchuan earthquake. This Western Sichuan Seismic Array (WSSA) was operational for more than 2 years and provides unique continuous recordings before, during and after the Wenchuan quake. The data obtained from WSSA were used to perform a series of studies related to the genesis and process of the Wenchuan earthquake, and the structure of the Eastern Tibetan Plateau [e.g., *Liu et al.*, 2009]. We use this data to investigate the change of crustal seismic velocity associated with the Wenchuan earthquake at the regional scale.

2. Data and Measurements of Relative Velocity Changes

[5] Our study area comprises the northern part of the WSSA (29° to 32° *N* and 100° to 105° *E*). We use 156 stations, with average station spacing of 20 ~ 30 km. Figure 1 shows the location of the stations and the main geological units in this area. The stations are distributed in the LMS, the Sichuan Basin (SB), the Songpan-Ganzi (SG) and Chuan-Dian (CD) blocks. The closest station is within 20 km of the epicenter of the Wenchuan earthquake.

[6] Seismic noise recorded from January 1, 2007 to the end of 2008 are used in this study. Some stations near the epicenter of the Wenchuan May 12, 2008 earthquake suffered power failure during the main shock. These stations were recovered after at most 15 days. For the stations in operation in the days following the event, it was verified on-site that they were functioning correctly. This dataset has long enough recordings before and after the earthquake to allow for the study of the crustal velocity changes. The following paragraphs present the different steps of the processing applied to measure the temporal seismic velocity changes.

[1]State Key Laboratory of Earthquake Dynamics, Institute of Geology, China Earthquake Administration, Beijing, China.
[2]Laboratoire de Géophysique Interne et de Tectonophysique, Université Joseph Fourier, CNRS, Grenoble, France.

0094-8276/10/2010GL044582

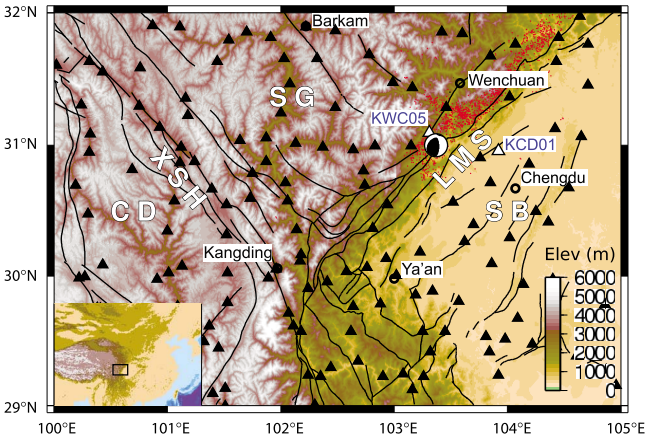

Figure 1. Stations used in this study (triangles). Black beach ball indicates the epicenter of the Wenchuan earthquake and red dots are aftershocks. Black lines are major faults in the studying region. SB, SG, CD, LMS and XSH stands for Sichuan basin, Songpan-Ganzi block, Chuan-Dian block, Longmen Shan fault zone and Xianshuihe fault zone respectively.

[7] Vertical component of the seismic records is used in this study. We first resample the data to 5 sps. A time domain normalization method is used to remove effects of strong localized energetic signal principally due to earthquakes and locally generated noise. The data preprocessing is the same as that of *Yao et al.* [2006]. We consider every possible station pairs with a spacing less than 200 km. We compute the NCFs of 30-day moving windows for periods between 1 and 3 seconds. We interpret the NCFs as an approximation of the actual Green function between the stations. The window duration of 30 days was chosen after testing the stability of the NCF versus window lengths. Figure 2 shows an example of the NCFs varying with time. It shows that the NCFs are well defined throughout the 2-year period. The direct wave amplitude shows seasonal variations that reflect changes in noise excitation. The coda waves show arrivals that remain stable over the whole 2-year period. In order to attenuate the effects of temporal variations in the distribution of the noise sources, we ignored the direct waves which are highly sensitive to azimuthal distribution of the noise intensity [e.g., *Froment et al.*, 2010]. We thus consider a window that starts long after the ballistic arrivals, which is about 25 s in Figure 2. We investigate travel time variations between NCFs using the coda of up to ±200 s lapse time. While calculating the NCFs, instrumental timing errors are checked by both the State-of-Health record of the instrument and by checking the time symmetry of the noise correlations [*Stehly et al.*, 2007]. Stations exhibiting instrumental timing problems have been removed.

[8] For each station pair, the NCFs stacked over the 2-year period of study defines the long-term reference trace. Travel time variation between the reference trace and each 30-day NCF is calculated with the doublet method. We thus obtain the delay δt in short moving windows centered at different lapse time τ in the coda. For a specific region and date, we average δt at lapse time τ over the station pairs, and a linear least-square regression is applied to get the relative travel time change ($\delta t/\tau$) for the specific date and region of interest. The relative velocity change is the opposite of the relative travel time change ($\delta v/v = -\delta t/\tau$).

3. Results

3.1. Temporal Velocity Changes

[9] The measurements of the velocity changes for groups of stations in the LMS fault belt, SG and SB blocks are shown in Figure 3. We note relatively weak and consistent velocity variation before the Wenchuan earthquake, sharp co-seismic velocity changes in LMS and SB, and attenuations after the earthquake. A long-term relaxation cannot be analyzed with the available records.

[10] The velocity fluctuation before the Wenchuan earthquake for the 3 regions is within ±0.02%. This is similar to what was observed before the Parkfield earthquake by *Brenguier et al.* [2008b].

[11] The temporal variations are different in the three regions (Figure 3). The seismic velocity drop reached a value about 0.08% just after the Wenchuan earthquake in the region close to the LMS fault. This is a bit larger, but of the same order as found for the M6.0 Parkfield earthquake [*Brenguier et al.*, 2008b]. Note that the network in Parkfield was just at the epicentral region with a spatial extension of about 20 km, which was of the order of the rupture size of the earthquake; WSSA has an aperture of about 300 km, which is also the length of the Wenchuan rupture. The similarity of the average change of velocity is probably a consequence of the earthquake scaling law with almost constant stress drop.

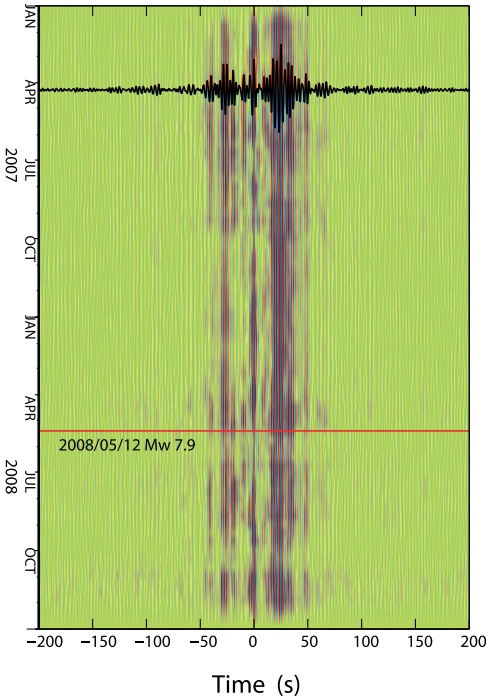

Figure 2. Thirty-day stacked NCFs for the station pair KWC05 and KCD01. The amplitude of the NCFs are in arbitrary unit. The distance between the 2 stations is 60.2 km, their positions are marked as open triangles and blue station names in Figure 1. The thick black curve represents the reference stacked NCF. The red line indicates the date of the Wenchuan earthquake.

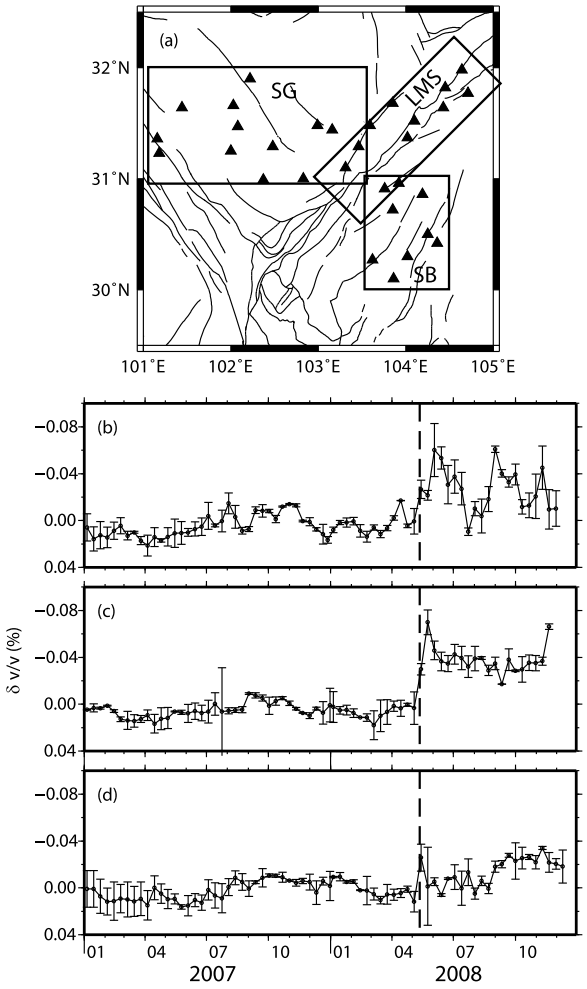

Figure 3. (a) Stations in 3 sub-regions and relative temporal velocity changes for the (b) SB, (c) LMS and (d) the SG block. Error bars correspond to uncertainty of the linear slope estimation of the relation delay δt versus lapse time τ. The vertical dashed line indicates the date of the Wenchuan Mw7.9 earthquake.

3.2. Spatial Distribution of the Co-seismic Velocity Changes

[12] The dense and nearly even spatial station distribution of the WSSA makes it possible to investigate the spatial distribution of velocity changes over the full region. To do this, we define a grid of 0.5° × 0.5° sub-regions. The stations considered for each small region are within 0.5° from the center of the region (see Figure S1 in auxiliary material).[1] Results are then interpolated to 0.25°. Note that we produce a smoothed regionalization, in agreement with the fact that we use coda waves with average lapse time of about 100 s that sample a wide zone. The co-seismic velocity change obtained for each of the sub-region is estimated as the difference between the velocities which were averaged over the period before the earthquake and over the 10-to-50-day period after. Figure 4 shows the spatial distribution of the estimated co-seismic velocity changes. Since the fluctuation of the measured velocity before the earthquake is ±0.02%, only regions where the co-seismic velocity change is larger than 0.02% are considered to have been affected by the earthquake.

[13] The velocity clearly dropped in a wide zone around the LMS, where the aftershocks are distributed. On the contrary, the crustal velocity hardly changed in the southern part of the LMS. Figure 4 shows that the velocity drop is similar on both sides of the fault, despite different geological characteristics of the two blocks.

[14] We evaluate the consistency of the velocity drop with the volumetric strain change associated with the earthquake. The strain is deduced from the kinematic model of *Shen et al.* [2009] based on joint inversion of co-seismic GPS and InSAR displacements (see Figure S2 of the auxiliary material). The map of velocity change has clear similarities with the dilatation distribution, which suggests that the two are causally related. At the regional scale, the velocity drop exhibits a better correlation with the dilatation than with the surface geology or the intensity map. We note that our smoothed regionalization prevents the detection of small scale variations.

4. Discussions and Conclusions

[15] This study demonstrates that, despite less rigorous station installation for this temporary network than for the permanent borehole stations of HRSN network in Parkfield, temporal velocity monitoring can be achieved with a similar resolution. We also show that the velocity change is detectable at the regional scale.

[16] Our results found a maximum velocity drop of 0.08% (or 4 times larger than the fluctuations before the main shock) just after the Wenchuan Mw 7.9 earthquake. The relative velocity change is only slightly larger than that of the 2004 Parkfield Mw 6.0 earthquake [*Brenguier et al.*, 2008b], which shows that the velocity change during an earthquake is not increasing with the total moment released. This probably results from the almost constant stress drop and strain change observed during earthquakes of various Mw. The velocity changes are found not only in the regions with sedimentary covers but also in the high plateau, showing that damage in the sedimentary cover is not the only cause of the temporal variations. The spatial distribution of the co-seismic velocity

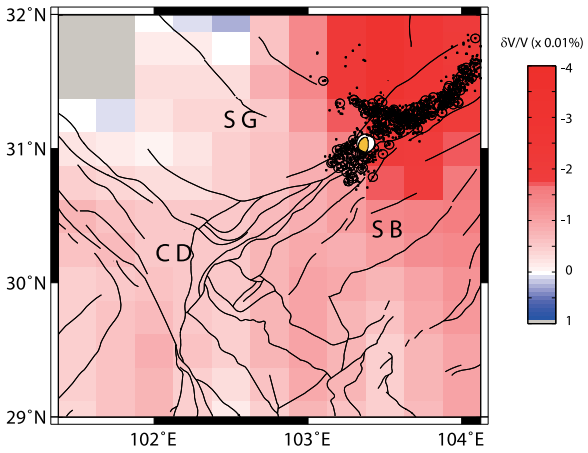

Figure 4. Distribution of co-seismic relative velocity changes. The beach ball indicates the epicenter of the Wenchuan earthquake, bold circles and small dots are aftershocks, thick lines are major faults in the region.

[1] Auxiliary materials are available in the HTML. doi:10.1029/2010GL044582.

changes is consistent with the distribution of volumetric strain change associated with the main shock.

[17] In this study we consider coda waves propagating, on average, for 100 s. For the region close to the LMS fault, these waves sample medium within a 150-km-radius zone around the fault. We evaluate the average volumetric strain change in this zone from the strain change produced by the rupture obtained by *Shen et al.* [2009] (Figure S2 of the auxiliary material). The average dilatation is about 2×10^{-6}, which corresponds to an average stress of 10^5 *Pa*. We thus infer a sensitivity of relative velocity change to stress on the order of 0.5×10^{-8} Pa^{-1}. This value should be compared to the direct measurement of *Niu et al.* [2008] at a depth of 1 km at SAFOD, that is 2.4×10^{-7} Pa^{-1}. Our observation is more than one order of magnitude smaller. This difference can be attributed to the fact that our measurements are sensitive to larger depths, where material can be expected to be less weathered or cracked, than the data used in the San Andreas fault study.

[18] **Acknowledgments.** The study was jointly supported by the Key Projects of Chinese National Programs for Fundamental Research and Development (2004CB418402), the National Natural Science Foundation of China (40974023) and the European Research Council (Advanced Grant Whisper). B.F. acknowledges financial support from Shell Research. Shuncheng Li, Biao Guo, Yu Li, Jun Wang and Shaohua Qi participated to the acquisition of field data. We thank Florent Brenguier, Céline Hadziioannou, Philippe Roux, Nikolai Shapiro, Huajian Yao and Rob van der Hilst for helpful discussions. We thank 2 anonymous reviewers for their helpful advises to improve this article.

References

Brenguier, F., N. M. Shapiro, M. Campillo, V. Ferrazzini, Z. Duputel, O. Coutant, and A. Nercessian (2008a), Towards forecasting volcanic eruptions using seismic noise, *Nat. Geosci.*, *1*, 126–130, doi:10.1038/ngeo104.

Brenguier, F., M. Campillo, C. Hadziioannou, N. M. Shapiro, R. M. Nadeau, and E. Larose (2008b), Postseismic relaxation along the San Andreas Fault at Parkfield from continuous seismological observations, *Science*, *321*, 1478–1481, doi:10.1126/science.1160943.

Burchfiel, B. C., L. H. Royden, R. D. van der Hilst, Z. Chen, R. W. King, C. Li, J. Lü, and H. Yao (2008), A geological and geophysical context for the Wenchuan earthquake of 12 May 2008, Sichuan, People's Republic of China, *GSA Today*, *18*(7), 4–11, doi:10.1130/GSATG18A.1.

Chen, J. H., Q. Y. Liu, S. C. Li, B. Guo, Y. Li, J. Wang, and S. H. Qi (2009), Seismotectonic study by relocation of the Wenchuan Ms 8.0 earthquake sequence (in Chinese), *Chin. J. Geophys.*, *52*(2), 390–397.

Froment, B., M. Campillo, P. Roux, P. Gouédard, A. Verdel, and R. Weaver (2010), Estimation of the effect of non-isotropically distributed energy on the apparent arrival time in correlations, *Geophysics*, in press.

Hadziioannou, C., E. Larose, O. Coutant, P. Roux, and M. Campillo (2009), Stability of monitoring weak changes in multiply scattering media with ambient noise correlation: Laboratory experiments, *J. Acoust. Soc. Am.*, *125*(6), 3688–3695, doi:10.1121/1.3125345.

Ji, C., and G. Hayes (2008), Preliminary result of the May 12, 2008 Mw 7.9 eastern Sichuan, China earthquake, U.S. Geol. Surv., Reston, Va. (Available at http://earthquake.usgs.gov/eqcenter/eqinthenews/2008/us2008ryan/finite_fault.php)

Liu, Q. Y., et al. (2009), Wenchuan Ms 8.0 earthquake: Preliminary study of the S-wave velocity structure of the crust and upper mantle (in Chinese), *Chin. J. Geophys.*, *52*(2), 309–319.

Niu, F., P. G. Silver, T. M. Daley, X. Cheng, and E. L. Majer (2008), Preseismic velocity changes observed from active source monitoring at the Parkfield SAFOD drill site, *Nature*, *454*, 204–208, doi:10.1038/nature07111.

Poupinet, G., W. L. Ellsworth, and J. Frechet (1984), Monitoring velocity variations in the crust using earthquake doublets: An application to the Calaveras Fault, California, *J. Geophys. Res.*, *89*, 5719–5731.

Sens-Schönfelder, C., and U. Wegler (2006), Passive image interferometry and seasonal variations of seismic velocities at Merapi Volcano, Indonesia, *Geophys. Res. Lett.*, *33*, L21302, doi:10.1029/2006GL027797.

Shapiro, N. M., and M. Campillo (2004), Emergence of broadband Rayleigh waves from correlations of the ambient seismic noise, *Geophys. Res. Lett.*, *31*, L07614, doi:10.1029/2004GL019491.

Shen, Z. K., et al. (2009), Slip maxima at fault junctions and rupturing of barriers during the 2008 Wenchuan earthquake, *Nat. Geosci.*, *2*, 718–724, doi:10.1038/ngeo636.

Stehly, L., M. Campillo, and N. M. Shapiro (2007), Traveltime measurements from noise correlations: Stability and detection of instrumental time-shifts, *Geophys. J. Int.*, *171*, 223–230, doi:10.1111/j.1365-246X.2007.03492.x.

Stehly, L., M. Campillo, B. Froment, and R. L. Weaver (2008), Reconstructing Green's function by correlation of the coda of the correlation (C3) of ambient seismic noise, *J. Geophys. Res.*, *113*, B11306, doi:10.1029/2008JB005693.

Wegler, U., H. Nakahara, C. Sens-Schönfelder, M. Korn, and K. Shiomi (2009), Sudden drop of seismic velocity after the 2004 Mw 6.6 mid-Niigata earthquake, Japan, observed with Passive Image Interferometry, *J. Geophys. Res.*, *114*, B06305, doi:10.1029/2008JB005869.

Xu, X. W., X. Z. Wen, G. H. Yu, G. H. Chen, Y. Klinger, J. Hubbard, and J. Shaw (2009), Coseismic reverse- and oblique-slip surface faulting generated by the 2008 Mw 7.9 Wenchuan earthquake, China, *Geology*, *37*(6), 515–518, doi:10.1130/G25462A.1.

Yao, H. J., R. D. van der Hilst, and M. V. de Hoop (2006), Surfave-wave array tomography in SE Tibet from ambient seismic noise and two-station analysis—I. Phase velocity maps, *Geophys. J. Int.*, *166*, 732–744.

Zhang, P. Z., X. Z. Wen, Z. K. Shen, and J. H. Chen (2010), Oblique, high-angle, listric-reverse faulting and associated development of strain: The Wenchuan earthquake of May 12, 2008, Sichuan, China, *Annu. Rev. Earth Planet. Sci.*, *38*,353–382, doi:10.1146/annurev-earth-040809-152602.

M. Campillo and B. Froment, Laboratoire de Géophysique Interne et de Tectonophysique, Université Joseph Fourier, CNRS, BP 53, F-38041 Grenoble CEDEX 9, France.

J. H. Chen and Q. Y. Liu, State Key Laboratory of Earthquake Dynamics, Institute of Geology, China Earthquake Administration, Beijing, 100029, China. (chenjh@ies.ac.cn)